This article has been accepted for publication in IEEE Communications Letters. This is the author's version which has not been fully edited and content may change prior to final publication. Citation information: DOI 10.1109/LCOMM.2022.3203521

Joint Precoder and Window Design for OFDM Sidelobe Suppression

Khawar Hussain, *Graduate Student Member, IEEE,* and Roberto López-Valcarce, *Senior Member, IEEE*

***Abstract*—Spectral precoding and windowing are two effective approaches to reduce out-of-band radiation (OBR) in multicarrier systems. Their performance comes at the price of reduced throughput and additional computational complexity, so there is strong motivation for simultaneously using both techniques. We present a novel design that jointly optimizes the precoder and window coefficients to minimize radiated power within a user-selectable frequency region. Results show that the proposed design achieves a better OBR/throughput/complexity tradeoff than either of these individual techniques separately.**

***Index Terms*—OFDM, out-of-band radiation, sidelobe suppression, windowing, spectral precoding.**

I. Introduction

Due to its inherent advantages, orthogonal frequency division multiplexing (OFDM) has established itself as the most popular multicarrier modulation scheme: it is spectrally efficient, robust against frequency-selective fading thanks to the cyclic prefix (CP), and well matched to multiple-input multiple-output (MIMO) operation [1]. Nevertheless, it has some drawbacks, including large spectrum sidelobes which cause high out-of-band radiation (OBR). To alleviate this issue, many techniques have been proposed, which can be broadly categorized as *frequency-domain* and *time-domain* methods.

Frequency-domain techniques suitably modify the samples at the input of the inverse fast Fourier transform (IFFT). Deactivating subcarriers near the band edges to shape the spectrum is simple but very inefficient, due to the high subcarrier sidelobes. Multiple choice sequence techniques [2], [3] require the transmission of side information with each symbol, increasing system overhead. Data-dependent techniques, such as constellation expansion [4] or subcarrier weighting [5], [6], are computationally expensive, as they require solving an optimization problem per OFDM symbol.

Spectral precoding is another frequency-domain approach to mitigate OBR, by which the transmitted sequence is computed as a linear combination of the data [7]–[11]. In general, precoding introduces distortion, so appropriate decoding is required at the receiver to avoid error rate degradation. If the precoding matrix has orthonormal columns, its effect can be easily inverted at the receiver without noise enhancement [9]–[11]. Nevertheless, orthogonal precoding (OP) generally suffers from high computational complexity. On the other hand, active interference cancellation (AIC) methods, which can be seen as a particular case of spectral precoding, use some reserved subcarriers for OBR reduction without altering the data subcarriers. Thus, AIC is transparent to the receiver, which merely discards the cancellation subcarriers [12], [13]. The complexity of AIC methods is significantly lower than that of OP, but at the expense of worse OBR performance. In both cases, additional subcarriers are required, with the corresponding impact on throughput.

Time-domain schemes modify the samples at the IFFT output. Standard filtering [14] is simple, but usually requires filters with long impulse responses, which decreases the effective guard interval of OFDM symbols. Data-dependent techniques like adaptive symbol transition [15] incur additional complexity, similarly to their frequency-domain counterparts. The typical rectangular pulse in CP-OFDM can be replaced by a pulse (or *window*) with soft edges, resulting in much sharper sidelobe decay in the frequency domain, a technique known as weighted overlap-add (WOLA) [16] or windowed OFDM (W-OFDM) [17]. The complexity of W-OFDM is low as compared to other OFDM-derived waveforms [18], but at the price of reduced efficiency due to the need to extend the symbol length. Different window functions are discussed in [19]. Among them, the raised cosine (RC) window is commonly used for its good performance and straightforward implementation [20]. The window can also be specifically tailored to minimize OBR over a desired range of frequencies [21].

Time- and frequency-domain approaches have their own advantages and drawbacks, and their tradeoffs involving OBR reduction, computational complexity, and throughput efficiency need not be the same. Such tradeoffs should improve by simultaneously acting in both domains; for example, a spectral precoder could be designed for a given window, as in [22]. Our goal is to further improve on such approach by *jointly* optimizing both precoder and window coefficients. Further differences between our design and [22] include: (i) we allow to target arbitrary frequency ranges by leveraging the design from [21] rather than using notch frequencies; (ii) we allow redundant spectral precoders, establishing the overall throughput efficiency once this redundancy is taken into account together with the symbol length extension due to windowing. The benefits of the proposed joint design, which is data-independent and can be computed offline, are illustrated for two particular precoding techniques which do not affect the bit error rate, namely OP and AIC.

II. System Model

Consider an OFDM signal generated with an IFFT of size N. Let $\mathcal{K} = \{k_1, k_2, \cdots, k_K\}$ denote the set of active subcarriers, and $x_k^{(m)}$ be the data modulated on the k-th subcarrier in the m-th symbol. The baseband samples of the multicarrier signal are then given by

$$s[n] = \sum_{m=-\infty}^{\infty} \sum_{k \in \mathcal{K}} x_k^{(m)} h_{\mathrm{P}}[n - mL] e^{\frac{2\pi}{N} k(n-mL)}, \quad (1)$$

The authors are with atlanTTic Research Center, Universidade de Vigo, 36310 Vigo, Spain (e-mail: {khawar, valcarce}@gts.uvigo.es)

This work was funded by MCIN/AEI/10.13039/501100011033 and FEDER "Una manera de hacer Europa" under project RODIN (PID2019-105717RB-C21/C22) and fellowship BES-2017-080305.

This article has been accepted for publication in IEEE Communications Letters. This is the author's version which has not been fully edited and content may change prior to final publication. Citation information: DOI 10.1109/LCOMM.2022.3203521

where L is the hop size in samples, and $h_{\rm P}[n]$ is the shaping pulse, with Fourier transform $H_{\rm P}(e^{j\omega}) = \sum_{n=-\infty}^{\infty} h_{\rm P}[n]e^{-j\omega n}$. The analog baseband signal is

$$s(t) = \sum_{n=-\infty}^{\infty} s[n]h_{\rm I}(t - nT_s), \tag{2}$$

where T_s is the sampling interval, and $h_{\rm I}(t)$ is the impulse response of the interpolation filter in the Digital-to-Analog Converter (DAC), with transform $H_{\rm I}(f) = \int_{-\infty}^{\infty} h_{\rm I}(t)e^{-j2\pi ft}{\rm d}t$. With $\Delta_f = \frac{1}{NT_s}$ the subcarrier spacing, let us define

$$\phi_k(f) \triangleq H_{\rm P}^*\left(e^{j2\pi(f-k\Delta_f)T_s}\right), \tag{3}$$

$$\boldsymbol{\phi}(f) \triangleq [\ \phi_{k_1}(f) \quad \phi_{k_2}(f) \quad \cdots \quad \phi_{k_K}(f)\ ]^T. \tag{4}$$

The pulse $h_{\rm P}[n]$ extends from $n = 0$ to $n = L+Q-1$, so that the first and the last Q samples of any consecutive symbols overlap. The central samples of $h_{\rm P}[n]$ are fixed to 1 to avoid distortion at the receiver: $h_{\rm P}[n] = 1$ for $Q \le n \le L-1$; whereas the edge samples $h_{\rm P}[n]$ for $n = 0, 1, \ldots, Q-1$ and $n = L, L+1, \ldots, L+Q-1$ are to be designed. The gradual transition from 0 to 1 results in a sharper PSD. On the other hand, the effective CP length is reduced to $N_{\rm CP} = L - N - Q$ samples due to the Q-sample overlap between consecutive symbols; therefore, for a given effective CP length (determined by the maximum expected length of the channel impulse response), windowing results in a throughput efficiency reduction by a factor $\frac{N+N_{\rm CP}}{N+N_{\rm CP}+Q}$.

III. Power Spectral Density

Let $\boldsymbol{d}_m \in \mathbb{C}^D$, with $D \le K$, be the data sequence to transmit. Each entry of $\boldsymbol{d}_m$ is independently drawn from an M-ary constellation $\mathcal{C}$ with zero mean and unit variance, so that $\mathbb{E}\{\boldsymbol{d}_m\} = \boldsymbol{0}$ and $\mathbb{E}\{\boldsymbol{d}_m\boldsymbol{d}_{m'}^H\} = \delta_{mm'}\boldsymbol{I}_D$. Thus, $R = K-D$ is the precoder redundancy. The vector of samples in the m-th block is denoted as

$$\boldsymbol{x}_m \triangleq [\ x_{k_1}^{(m)} \quad x_{k_2}^{(m)} \quad \cdots \quad x_{k_K}^{(m)}\ ]^T. \tag{5}$$

We consider linear memoryless precoding, for which $\{\boldsymbol{x}_m\}$ is generated from $\{\boldsymbol{d}_m\}$ as

$$\boldsymbol{x}_m = \boldsymbol{G}\boldsymbol{d}_m, \tag{6}$$

where $\boldsymbol{G} \in \mathbb{C}^{K\times D}$ is the precoding matrix. Then, as shown in [23], the power spectral density (PSD) of $s(t)$ is given by

$$S_s(f) = \frac{|H_{\rm I}(f)|^2}{LT_s}\boldsymbol{\phi}^H(f)\boldsymbol{G}\boldsymbol{G}^H\boldsymbol{\phi}(f). \tag{7}$$

Note that $\boldsymbol{\phi}(f)$ in (4) can be rewritten as $\boldsymbol{\phi}(f) = \boldsymbol{M}(f)\boldsymbol{h}$, where $\boldsymbol{M}(f) \in \mathbb{C}^{K\times(L+Q)}$ is given entrywise by

$$[\boldsymbol{M}(f)]_{pq} = e^{j2\pi(q-1)(f-k_p\Delta_f)}, \quad \begin{cases} 1 \le p \le K, \\ 1 \le q \le L+Q, \end{cases} \tag{8}$$

and $\boldsymbol{h} \in \mathbb{C}^{L+Q}$ comprises the (conjugated) pulse samples:

$$\boldsymbol{h} \triangleq [\ h^*[0] \quad h^*[1] \quad \cdots \quad h^*[L+Q-1]\ ]^T. \tag{9}$$

Thus, $S_s(f)$ in (7) can be rewritten in terms of $\boldsymbol{G}$ and $\boldsymbol{h}$ as

$$S_s(f) = \frac{|H_{\rm I}(f)|^2}{LT_s}\boldsymbol{h}^H\boldsymbol{M}^H(f)\boldsymbol{G}\boldsymbol{G}^H\boldsymbol{M}(f)\boldsymbol{h}. \tag{10}$$

IV. Joint Precoder and Window Design

Let $W(f) \ge 0$ be a weighting function, giving emphasis to those frequencies over which PSD reduction is important. Then, the weighted power, which quantifies OBR, is given by

$$\mathcal{P}_{\rm W} = \int_{-\infty}^{\infty} W(f)S_s(f){\rm d}f. \tag{11}$$

The goal is to minimize $\mathcal{P}_{\rm W}$ with respect to the pulse $\boldsymbol{h}$ and precoder $\boldsymbol{G}$. This general problem can be stated as

$$\min_{\boldsymbol{h},\boldsymbol{G}} \mathcal{P}_{\rm W}(\boldsymbol{h},\boldsymbol{G}) \ \text{ s. to } \begin{cases} h[n] = 1, \ \ Q \le n \le L-1, \\ \text{structural constraint on } \boldsymbol{G}. \end{cases} \tag{12}$$

The second constraint in (12) depends on the particular precoder structure (*e.g.,* OP or AIC) as discussed below.

Problem (12) is nonconvex in general. However, if either $\boldsymbol{h}$ or $\boldsymbol{G}$ is fixed, the corresponding subproblem becomes manageable. Thus, we propose to cyclically minimize $\mathcal{P}_{\rm W}$ with respect to these parameters (pulse and precoder).

A. Optimal window for a given precoder

For fixed $\boldsymbol{G}$, the weighted power in (11) becomes $\mathcal{P}_{\rm W} = \boldsymbol{h}^H\boldsymbol{Z}(\boldsymbol{G})\boldsymbol{h}$, where $\boldsymbol{Z}(\boldsymbol{G}) \in \mathbb{C}^{(L+Q)\times(L+Q)}$ is given by

$$\boldsymbol{Z}(\boldsymbol{G}) \triangleq \int_{-\infty}^{\infty} W(f)\frac{|H_{\rm I}(f)|^2}{LT_s}\boldsymbol{M}^H(f)\boldsymbol{G}\boldsymbol{G}^H\boldsymbol{M}(f){\rm d}f, \tag{13}$$

which is Hermitian positive (semi-)definite. Then the following convex subproblem is obtained:

$$\min_{\boldsymbol{h}} \boldsymbol{h}^H\boldsymbol{Z}(\boldsymbol{G})\boldsymbol{h} \quad \text{s. to} \quad \boldsymbol{J}^H\boldsymbol{h} = \boldsymbol{1}, \tag{14}$$

where $\boldsymbol{J} \in \mathbb{C}^{(L+Q)\times(L-Q)}$ comprises columns $Q+1$ through L of $\boldsymbol{I}_{L+Q}$, and $\boldsymbol{1} \in \mathbb{C}^{L-Q}$ is the all-ones vector. The solution to (14) can be readily found in closed form: letting $\widetilde{\boldsymbol{J}} \in \mathbb{C}^{(L+Q)\times 2Q}$ comprise columns 1 through Q and $L+1$ through $L+Q$ of $\boldsymbol{I}_{L+Q}$, then $\widetilde{\boldsymbol{J}}^H\boldsymbol{h}$ contains the edge samples of $\boldsymbol{h}$, given by $\widetilde{\boldsymbol{J}}^H\boldsymbol{h} = -(\widetilde{\boldsymbol{J}}^H\boldsymbol{Z}(\boldsymbol{G})\widetilde{\boldsymbol{J}})^{-1}\widetilde{\boldsymbol{J}}^H\boldsymbol{Z}(\boldsymbol{G})\boldsymbol{J}\boldsymbol{1}$.

B. Optimal precoder for a given window

The PSD from (10) can be rewritten as

$$S_s(f) = {\rm tr}\{\boldsymbol{G}^H\boldsymbol{\Phi}(f;\boldsymbol{h})\boldsymbol{G}\}, \tag{15}$$

where $\boldsymbol{\Phi}(f;\boldsymbol{h}) \triangleq \frac{|H_I(f)|^2}{LT_s}\boldsymbol{M}(f)\boldsymbol{h}\boldsymbol{h}^H\boldsymbol{M}^H(f)$. Thus, letting $\boldsymbol{A}_{\rm W}(\boldsymbol{h}) \triangleq \int_{-\infty}^{\infty} W(f)\boldsymbol{\Phi}(f;\boldsymbol{h}){\rm d}f$, $\mathcal{P}_{\rm W}$ in (11) becomes

$$\mathcal{P}_{\rm W} = {\rm tr}\{\boldsymbol{G}^H\boldsymbol{A}_{\rm W}(\boldsymbol{h})\boldsymbol{G}\}. \tag{16}$$

1) Orthogonal precoder: With OP, the structural constraint on the precoder reads as $\boldsymbol{G}^H\boldsymbol{G} = \boldsymbol{I}_D$, yielding

$$\min_{\boldsymbol{G}} {\rm tr}\{\boldsymbol{G}^H\boldsymbol{A}_{\rm W}(\boldsymbol{h})\boldsymbol{G}\} \quad \text{s. to} \quad \boldsymbol{G}^H\boldsymbol{G} = \boldsymbol{I}_D, \tag{17}$$

whose solution $\boldsymbol{G}$ comprises the eigenvectors of $\boldsymbol{A}_{\rm W}(\boldsymbol{h})$ corresponding to the D smallest eigenvalues.

This article has been accepted for publication in IEEE Communications Letters. This is the author's version which has not been fully edited and content may change prior to final publication. Citation information: DOI 10.1109/LCOMM.2022.3203521

2) AIC precoder: The data vector $\boldsymbol{d}_m$ is directly mapped to D of the K active subcarriers, whereas the remaining $R = K - D$ subcarriers are used for cancellation. Let $\boldsymbol{S} \in \mathbb{C}^{K\times D}$ comprise the D columns of $\boldsymbol{I}_K$ corresponding to the indices of active subcarriers to which the data is directly mapped, and let $\boldsymbol{T} \in \mathbb{C}^{K\times(K-D)}$ comprise the remaining $K-D$ columns of $\boldsymbol{I}_K$. Then the structural constraint on the AIC precoder is $\boldsymbol{G} = \boldsymbol{S}+\boldsymbol{T}\boldsymbol{\Theta}$, where $\boldsymbol{S}$, $\boldsymbol{T}$ are fixed whereas $\boldsymbol{\Theta} \in \mathbb{C}^{(K-D)\times D}$ is a free parameter. Minimizing $\mathcal{P}_{\rm W} = \mathrm{tr}\{(\boldsymbol{S}+\boldsymbol{T}\boldsymbol{\Theta})^H \boldsymbol{A}_{\rm W}(\boldsymbol{h})(\boldsymbol{S}+\boldsymbol{T}\boldsymbol{\Theta})\}$ w.r.t. $\boldsymbol{\Theta}$ is a convex quadratic problem with solution $\boldsymbol{\Theta} = -(\boldsymbol{T}^H\boldsymbol{A}_{\rm W}(\boldsymbol{h})\boldsymbol{T})^{-1}\boldsymbol{T}\boldsymbol{A}_{\rm W}(\boldsymbol{h})\boldsymbol{S}$. However, this may result in too much power being allocated to cancellation subcarriers, resulting in undesirably large PSD peaks. To control the size of these peaks, a regularization term can be introduced, leading to the following subproblem:

$$\min_{\boldsymbol{\Theta}} \mathrm{tr}\{(\boldsymbol{S}+\boldsymbol{T}\boldsymbol{\Theta})^H \boldsymbol{A}_{\rm W}(\boldsymbol{h})(\boldsymbol{S}+\boldsymbol{T}\boldsymbol{\Theta})\} + \gamma\|\boldsymbol{\Theta}\|_F^2, \quad (18)$$

where larger values of the regularization parameter $\gamma \geq 0$ will result in lower spectral peaks. The solution to (18) is given by $\boldsymbol{\Theta} = -(\boldsymbol{T}^H\boldsymbol{A}_{\rm W}(\boldsymbol{h})\boldsymbol{T} + \gamma\boldsymbol{I}_R)^{-1}\boldsymbol{T}\boldsymbol{A}_{\rm W}(\boldsymbol{h})\boldsymbol{S}$.

C. Cyclic optimization

To obtain an approximate solution to (12), we first initialize $\boldsymbol{h}_0$ as an RC window. Then, for $k \geq 1$, we solve:

$$\begin{aligned} \text{OP:}\quad \boldsymbol{G}_k &= \arg\min_{\boldsymbol{G}} \mathcal{P}_{\rm W}(\boldsymbol{h}_{k-1}, \boldsymbol{G}) \\ &\quad \text{s. to}\quad \boldsymbol{G}^H\boldsymbol{G} = \boldsymbol{I}_D \quad (19) \\ \text{AIC:}\quad \boldsymbol{G}_k &= \arg\min_{\boldsymbol{G}} \mathcal{P}_{\rm W}(\boldsymbol{h}_{k-1}, \boldsymbol{G}) + \gamma\|\boldsymbol{\Theta}\|_F^2 \\ &\quad \text{s. to}\quad \boldsymbol{G} = \boldsymbol{S}+\boldsymbol{T}\boldsymbol{\Theta} \quad (20) \\ \text{OP \& AIC:}\quad \boldsymbol{h}_k &= \arg\min_{\boldsymbol{h}} \mathcal{P}_{\rm W}(\boldsymbol{h}, \boldsymbol{G}_k) \\ &\quad \text{s. to}\quad \boldsymbol{J}^H\boldsymbol{h} = \boldsymbol{1}. \quad (21) \end{aligned}$$

Note that the sequence of objective values $\mathcal{P}_{\rm W}(\boldsymbol{h}_k, \boldsymbol{G}_k)$ for OP, or $\mathcal{P}_{\rm W}(\boldsymbol{h}_k, \boldsymbol{G}_k)+\gamma\|\boldsymbol{\Theta}_k\|_F^2$ for AIC, is non-increasing and bounded below, so it must be convergent. Although there is no guarantee that the global optimum of (12) is found, simulation results validate the good performance of the proposed scheme.

V. Receiver operation, Efficiency, and Complexity

At the receiver end, after synchronization, the CP and the Q overlapping samples between consecutive blocks are removed. After an N-point FFT and equalization, the vector $\boldsymbol{r} \in \mathbb{C}^K$ with the samples of active subcarriers is obtained. With OP, data can be estimated as $\mathrm{DEC}\{\boldsymbol{G}^H\boldsymbol{r}\}$, where $\mathrm{DEC}\{\cdot\}$ is an entrywise operator returning, for each entry, the closest symbol in the constellation; since $\boldsymbol{G}$ has orthonormal columns, noise enhancement is avoided. On the other hand, AIC is transparent to the receiver: data can be estimated as $\mathrm{DEC}\{\boldsymbol{S}^H\boldsymbol{r}\}$, *i.e.,* cancellation subcarriers are simply discarded.

Each OFDM block, carrying D data symbols, is sent every LT_s seconds, so that the bit rate is $R_b = \frac{D}{LT_s} = \frac{(K-R)\log_2 M}{(N+N_{\rm CP}+Q)T_s}$ bits/s. For the same effective CP length $N_{\rm CP}$, the baseline is given by a system with no precoding ($R = 0$) and without windowing ($Q = 0$), whose corresponding bit rate is $R_{b,\rm ref} = \frac{K\log_2 M}{(N+N_{\rm CP})T_s}$ bits/s. Hence, the metric for throughput efficiency is

$$\eta = \frac{R_b}{R_{b,\rm ref}} = \frac{1-R/K}{1+Q/(N_{\rm CP}+N)}, \quad (22)$$

which depends on the relative precoder redundancy $\frac{R}{K}$ and the relative window redundancy $\frac{Q}{N_{\rm CP}+N}$. Thus, a given efficiency η can be achieved with different (R, Q) values, by using longer windows with fewer redundant subcarriers, or vice versa.

The proposed design is data-independent, so it can be computed offline. Regarding online complexity, windowing takes $2Q$ complex multiplications per OFDM symbol (cm/symb) at the transmitter, whereas no additional complexity is incurred at the receiver; with respect to the precoder, one has:

- **OP.** The online complexity at each of transmitter and receiver is $K(K-R)$ cm/symb, if multiplication by $\boldsymbol{G}$ or $\boldsymbol{G}^H$ is implemented directly, but it becomes $R(2K-R)$ cm/symb with Clarkson's reduced complexity approach [24], which will be assumed in the sequel. With this, the total complexity including windowing and precoding is $2R(2K-R)+2Q$ cm/symb.
- **AIC.** At the transmitter, AIC requires $R(K-R)$ cm/symb. At the receiver end, the R cancellation subcarriers are just discarded, with no additional complexity. The total complexity is thus $R(K-R)+2Q$ cm/symb.

VI. Results

We study the performance of the proposed *joint precoder and window* (JPW) design in a CP-OFDM system with IFFT size $N = 256$ and CP length $N_{\rm CP} = N/4$. The DAC filter is lowpass with $H_{\rm I}(f) = 1$ for $|f| \leq \frac{1}{2T_s}$ and zero otherwise. There are $K = 65$ active subcarriers, located symmetrically about the carrier frequency. The weighting function is $W(f) = 1, \forall\left\{\frac{1}{8T_s} + \frac{\Delta_f}{2} \leq |f| \leq \frac{1}{2T_s}\right\}$, and zero otherwise.

A. Windowing and Orthogonal Precoding

For a given efficiency η, JPW provides the flexibility to trade off complexity and OBR reduction by choosing R and Q. Fig. 1 shows the PSD obtained by JPW with orthogonal precoding (JPW-OP), along with that of standard CP-OFDM with 5 null subcarriers at each band edge, for the above system parameters and fixing $\eta = 84.6\%$. Note that $(R, Q) = (10, 0)$ corresponds to orthogonal precoding with rectangular pulses, whereas $(R, Q) = (0, 58)$ reduces to the optimal window design from [21] with no precoding. It is seen that windowing, by itself, is unable to provide a fast rolloff at the passband edge; an orthogonal precoder, without windowing, performs much better in this regard, but the associated online complexity is significantly higher. The tradeoff provided by JPW-OP is clearly seen in Fig. 1, and also in Table I. For $(R, Q) = (8, 12)$, JPW-OP provides a 4.3-dB OBR improvement with respect to the standard orthogonal precoder, with 82.3% of its complexity. With $(R, Q) = (6, 23)$, complexity can be reduced to 63.9%, with just a small OBR degradation of 0.5 dB.

Table I also shows the results for a simplified design in which the window is fixed to an RC pulse, and then the orthogonal precoder is optimized for this fixed window, as

This article has been accepted for publication in IEEE Communications Letters. This is the author's version which has not been fully edited and content may change prior to final publication. Citation information: DOI 10.1109/LCOMM.2022.3203521

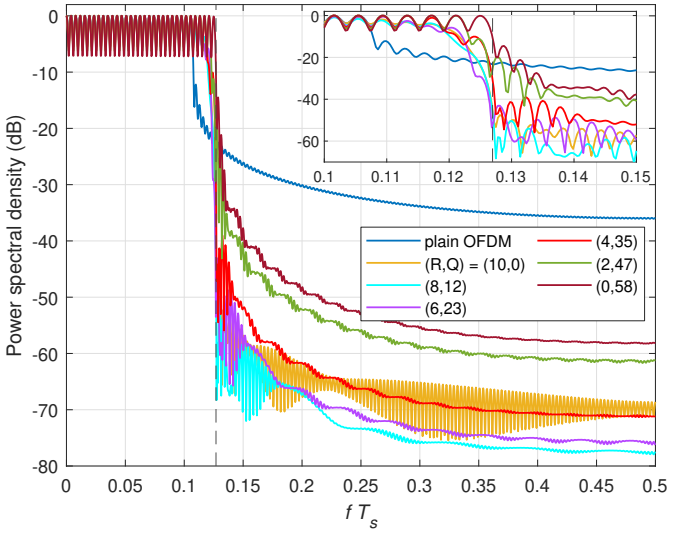

Fig. 1. PSD of the proposed JPW-OP design for different (R, Q) pairs. $\eta = 84.6\%$, $N = 256$, $N_{\mathrm{CP}} = N/4$, $K = 65$.

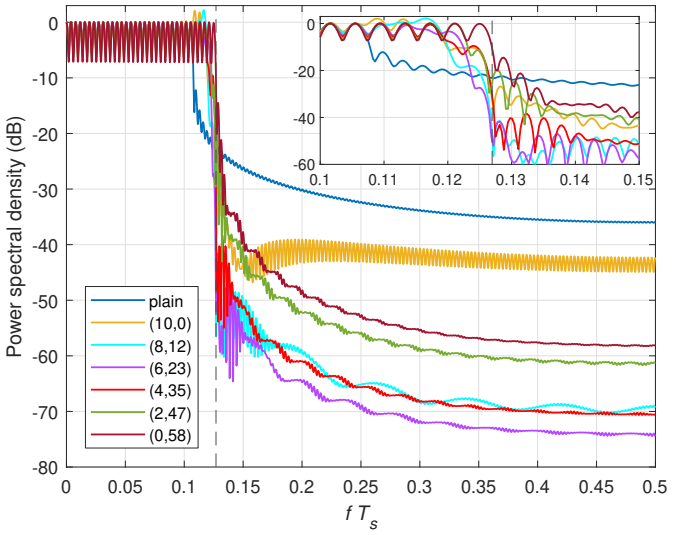

Fig. 2. PSD of JPW-AIC for different (R, Q) pairs. $\eta = 84.6\%$. Spectral peak is limited to 2 dB. $N = 256$, $N_{\mathrm{CP}} = N/4$, $K = 65$.

proposed in [22]. This approach, termed "RC-OP", corresponds to performing (19) for iteration $k = 1$ of the JPW-OP design, and then stopping. (We denote "RC-AIC" the analogous strategy for AIC precoders). Whereas JPW-OP and RC-OP have the same online complexity for a given (R, Q) pair, it is seen that jointly optimizing the precoder and the pulse improves OBR performance, *e.g.,* by 5.5 dB for $(R, Q) = (8, 12)$. Nevertheless, the RC-OP design may be attractive in dynamic spectrum access scenarios requiring frequent recomputation of precoder and window parameters due to the varying availability of spectral subbands.

B. Windowing and AIC precoding

In addition to being transparent to the receiver, AIC is computationally much simpler than orthogonal precoding. Thus, the online complexity of JPW with AIC precoding

TABLE I
ONLINE COMPLEXITY AND OBR (RELATIVE TO THAT OF PLAIN CP-OFDM WITH 10 NULL SUBCARRIERS) OF JPW-OP AND RC-OP. $\eta = 84.6\%$.

(R, Q)	$(10, 0)$	$(8, 12)$	$(6, 23)$	$(4, 35)$	$(2, 47)$	$(0, 58)$
cm/symb	2400 100%	1976 82.3%	1534 63.9%	1078 44.9%	606 25.2%	116 4.8%
OBR, dBr JPW-OP RC-OP	 −31.8 −31.8	 −36.1 −30.6	 −31.3 −28.9	 −24.1 −22.8	 −10.6 −9.0	 −3.9 −2.8

TABLE II
ONLINE COMPLEXITY AND OBR (RELATIVE TO THAT OF PLAIN CP-OFDM WITH 10 NULL SUBCARRIERS) OF JPW-AIC AND RC-AIC. $\eta = 84.6\%$, SPECTRAL PEAK ≤ 2 dB.

(R, Q)	$(10, 0)$	$(8, 12)$	$(6, 23)$	$(4, 35)$	$(2, 47)$	$(0, 58)$
cm/symb	550 100%	480 87.3%	400 72.7%	314 57%	220 40%	116 21%
OBR, dBr JPW-AIC RC-AIC	 −9.9 −9.9	 −28.3 −26.5	 −29.8 −27.8	 −23.6 −22.2	 −10.6 −9.0	 −3.9 −2.8

(JPW-AIC) is significantly lower than that of JPW-OP. Fig. 2 shows the corresponding PSDs for $\eta = 84.6\%$. In each case, half of the R cancellation subcarriers are placed at each of the passband edges, and the regularization parameter γ is adjusted to prevent spectral peaks above 2 dB. It is seen that both AIC precoding without windowing, *i.e.,* $(R, Q) = (10, 0)$, and windowing without precoding, *i.e.,* $(R, Q) = (0, 58)$, present serious limitations in terms of sidelobe suppression. By suitably choosing (R, Q), performance can be significantly improved, as seen in Fig. 2 and Table II. As a side benefit, for $R \leq 6$, the joint use of windowing and precoding turns out to avoid spectral peaks altogether in this case. Fig. 3 shows the convergence of the cyclic scheme (19)-(21) in this setting.

Interestingly, JPW-AIC may be able to provide OBR reduction levels comparable to those obtained with the standard (*i.e.,* no windowing) orthogonal precoder, with much less online

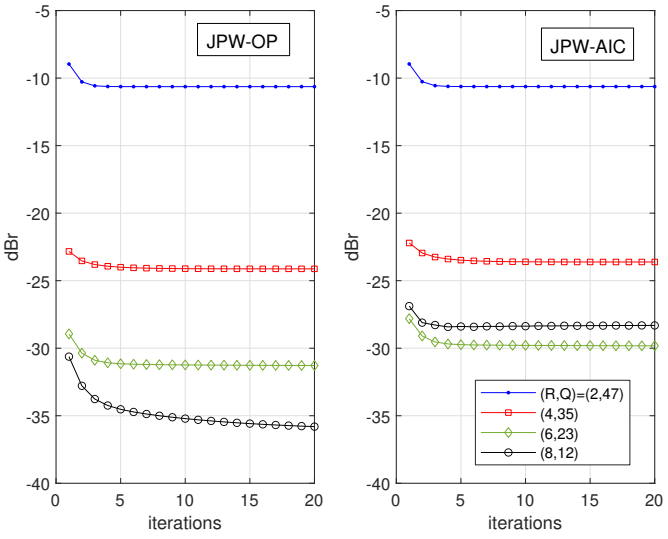

Fig. 3. Convergence of the proposed designs in terms of OBR in the setting of Figs. 1 and 2.

This article has been accepted for publication in IEEE Communications Letters. This is the author's version which has not been fully edited and content may change prior to final publication. Citation information: DOI 10.1109/LCOMM.2022.3203521

TABLE III
ONLINE COMPLEXITY AND OBR (RELATIVE TO PLAIN OFDM WITH NULL SUBCARRIERS) OF DIFFERENT DESIGNS. $N = 256$, $K = 65$.

η	90.8%		87.7%		84.6%		81.5%		78.5%	
$N_{\mathrm{CP}} = N/4$	cm/symb	dBr	cm/symb	dBr	cm/symb	dBr	cm/symb	dBr	cm/symb	dBr
OP (R)	1488 (6)	-14.5	1952 (8)	-22.8	2400 (10)	-31.8	2832 (12)	-41.4	3248 (14)	-51.1
AIC (R)	354 (6)	-6.3	456 (8)	-7.9	550 (10)	-9.8	636 (12)	-11.5	714 (14)	-13.3
W-OFDM (Q)	33 (16)	-1.8	90 (45)	-3.2	116 (58)	-3.9	144 (72)	-4.7	176 (88)	-5.6
RC-OP (R, Q)	1030 (4,11)	-14.5	1510 (6,11)	-23.5	1976 (8,12)	-30.6	2424 (10,12)	-33.0	2858 (12,13)	-37.2
JPW-OP (R, Q)		-15.6		-24.6		-36.1		-47.1		-49.2
RC-AIC (R, Q)	266 (4,11)	-12.7	376 (6,11)	-20.9	400 (6,23)	-27.8	504 (8,24)	-31.1	530 (8,37)	-32.3
JPW-AIC (R, Q)		-14.2		-22.3		-29.8		-42.1		-50.8
$N_{\mathrm{CP}} = N/16$	cm/symb	dBr	cm/symb	dBr	cm/symb	dBr	cm/symb	dBr	cm/symb	dBr
OP (R)	1488 (6)	-18.3	1952 (8)	-27.1	2400 (10)	-37.7	2832 (12)	-50.5	3248 (14)	-67.6
AIC (R)	354 (6)	-3.5	456 (8)	-4.5	550 (10)	-5.4	636 (12)	-6.9	714 (14)	-7.8
W-OFDM (Q)	56 (28)	-1.9	76 (38)	-2.4	98 (49)	-3.1	124 (62)	-3.9	150 (75)	-4.7
RC-OP (R, Q)	1026 (4,9)	-14.0	1508 (6,10)	-27.1	1528 (6,20)	-30.6	1994 (8,21)	-32.9	2442 (10,21)	-37.7
JPW-OP (R, Q)		-15.3		-29.0		-35.5		-46.0		-60.3
RC-AIC (R, Q)	262 (4,9)	-9.4	282 (4,19)	-14.5	394 (6,20)	-21.2	416 (6,31)	-30.4	440 (6,43)	-31.7
JPW-AIC (R, Q)		-11.1		-16.4		-23.3		-35.4		-42.2

complexity. From Tables I and II, it is seen that for the same efficiency ($\eta = 84.6\%$), JPW-AIC with $(R, Q) = (6, 23)$ performs only 2 dB worse than the standard orthogonal precoder, with just $\frac{400}{2400} = 16.7\%$ of the complexity (which is all placed at the transmitter). This is further illustrated in Table III, which shows the results obtained in this setting for two CP lengths ($N/4$ and $N/16$) and for different efficiency values, and where we have picked the pair (R, Q) corresponding to the largest OBR reduction for JPW-OP and JPW-AIC in each case. For all AIC-based schemes, spectral peaks are kept below 2 dB.

VII. CONCLUSION

Energy efficiency is a critical aspect of wireless transceivers, and thus it is important to exploit all available tools at one's disposal to perform a given task with the lowest energy consumption. We have shown that, for multicarrier systems, the combination of spectral precoding and windowing has the potential to provide sidelobe suppression comparable to that of standard precoding while sustaining the same throughput, but with much less online complexity. The proposed design for jointly computing precoder and window coefficients can be run offline, and it can be flexibly adapted to emphasize suppression over a user-selectable frequency range.

REFERENCES

[1] Y. Li and G. Stüber, Eds., *Orthogonal Frequency Division Multiplexing for Wireless Communications.* Boston, MA, USA: Springer, 2006.

[2] I. Cosovic and V. Janardhanam, "Sidelobe suppression in OFDM systems," in *Multi-Carrier Spread-Spectrum*, K. Fazel and S. Kaiser, Eds. Dordrecht: Springer Netherlands, 2006, pp. 473–482.

[3] I. Cosovic and T. Mazzoni, "Suppression of sidelobes in OFDM systems by multiple-choice sequences," *Eur. Trans. Telecomm.*, vol. 17, pp. 623–630, 2006.

[4] S. Pagadarai, R. Rajbanshi, A. M. Wyglinski, and G. J. Minden, "Sidelobe suppression for OFDM-based cognitive radios using constellation expansion," in *IEEE Wireless Commun. Netw. Conf.*, 2008, pp. 888–893.

[5] I. Cosovic, S. Brandes, and M. Schnell, "Subcarrier weighting: a method for sidelobe suppression in OFDM systems," *IEEE Commun. Lett.*, vol. 10, no. 6, pp. 444–446, Jun. 2006.

[6] R. Kumar and A. Tyagi, "Extended subcarrier weighting for sidelobe suppression in OFDM based cognitive radio," *Wireless Pers. Commun.*, vol. 87, no. 3, pp. 779–796, Apr. 2016. [Online]. Available: https://doi.org/10.1007/s11277-015-2623-8

[7] C.-D. Chung, "Spectrally precoded OFDM," *IEEE Trans. Commun.*, vol. 54, no. 12, pp. 2173–2185, Dec. 2006.

[8] J. van de Beek, "Sculpting the multicarrier spectrum: a novel projection precoder," *IEEE Commun. Lett.*, vol. 13, no. 12, pp. 881–883, Dec. 2009.

[9] R. Xu and M. Chen, "A precoding scheme for DFT-based OFDM to suppress sidelobes," *IEEE Commun. Lett.*, vol. 13, no. 10, pp. 776–778, Oct. 2009.

[10] M. Ma, X. Huang, B. Jiao, and Y. J. Guo, "Optimal orthogonal precoding for power leakage suppression in DFT-based systems," *IEEE Trans. Commun.*, vol. 59, no. 3, pp. 844–853, Mar. 2011.

[11] R. Kumar, K. Hussain, and R. López-Valcarce, "Mask-compliant orthogonal precoding for spectrally efficient OFDM," *IEEE Trans. Commun.*, vol. 69, no. 3, pp. 1990–2001, 2021.

[12] S. Brandes, I. Cosovic, and M. Schnell, "Reduction of out-of-band radiation in OFDM systems by insertion of cancellation carriers," *IEEE Commun. Lett.*, vol. 10, no. 6, pp. 420–422, Jun. 2006.

[13] J. F. Schmidt, S. Costas-Sanz, and R. López-Valcarce, "Choose your subcarriers wisely: Active interference cancellation for cognitive OFDM," *IEEE J. Emerg. Sel. Topics Circuits Syst.*, vol. 3, no. 4, pp. 615–625, Dec. 2013.

[14] M. Faulkner, "The effect of filtering on the performance of OFDM systems," *IEEE Trans. Veh. Technol.*, vol. 49, no. 5, pp. 1877–1884, 2000.

[15] H. A. Mahmoud and H. Arslan, "Sidelobe suppression in OFDM-based spectrum sharing systems using adaptive symbol transition," *IEEE Commun. Lett.*, vol. 12, no. 2, pp. 133–135, Feb. 2008.

[16] R. Zayani, Y. Medjahdi, H. Shaiek, and D. Roviras, "WOLA-OFDM: A potential candidate for asynchronous 5G," in *2016 IEEE Global Commun. Workshops*, Dec 2016, pp. 1–5.

[17] A. A. Zaidi, R. Baldemair, H. Tullberg, H. Bjorkegren, L. Sundstrom, J. Medbo, C. Kilinc, and I. Da Silva, "Waveform and numerology to support 5G services and requirements," *IEEE Commun. Mag.*, vol. 54, no. 11, pp. 90–98, Nov. 2016.

[18] S. Lien, S. Shieh, Y. Huang, B. Su, Y. Hsu, and H. Wei, "5G new radio: Waveform, frame structure, multiple access, and initial access," *IEEE Commun. Mag.*, vol. 55, no. 6, pp. 64–71, June 2017.

[19] B. Farhang-Boroujeny, "OFDM versus filter bank multicarrier," *IEEE Signal Process. Mag.*, vol. 28, no. 3, pp. 92–112, May 2011.

[20] D. R1-162199, "Waveform candidates," Qualcomm Inc., Busan, South Korea, Apr. 2016.

[21] K. Hussain and R. López-Valcarce, "Optimal window design for W-OFDM," in *IEEE Int. Conf. Acoust., Speech, Signal Process. (ICASSP)*, 2020, pp. 5275–5289.

[22] T. Taheri, R. Nilsson, and J. van de Beek, "Hybrid spectral precoding/windowing for low-latency OFDM," in *IEEE Veh. Technol. Conf. (VTC Spring)*, 2017.

[23] R. López-Valcarce, "General form of the power spectral density of multicarrier signals," *IEEE Commun. Lett.*, accepted.

[24] I. V. L. Clarkson, "Orthogonal precoding for sidelobe suppression in DFT-based systems using block reflectors," in *IEEE Int. Conf. Acoust., Speech, Signal Process.*, 2017, pp. 3709–3713.